● RESEARCH ARTICLE

Establishment of a rat model of chronic thoracolumbar cord compression with a flat plastic screw

Yong Sun[1], Li-hai Zhang[1], Yang-mu Fu[1], Zhi-rui Li[1], Jian-heng Liu[1], Jiang Peng[2], Bin Liu[2], Pei-fu Tang[1,*]

1 Department of Orthopedics, Chinese PLA General Hospital, Beijing, China
2 Department of Orthopedics Research Institute, Chinese PLA General Hospital, Beijing, China

Graphical Abstract

Progressive screw insertion can successfully establish a rat model of chronic thoracolumbar cord compression
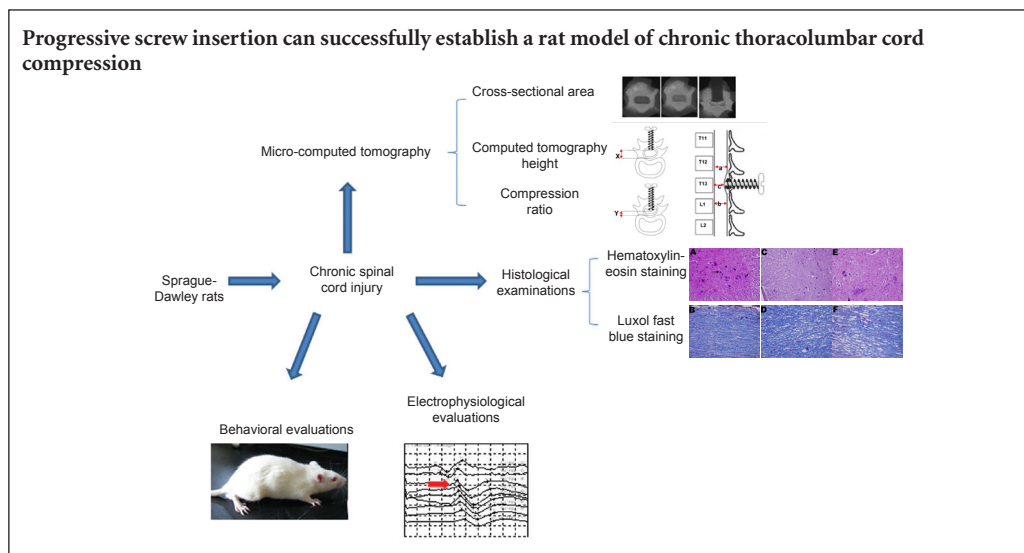
Correspondence to:
Pei-fu Tang, M.D.,
pftang301@163.com.

orcid:
0000-0003-4279-1704
(Pei-fu Tang)

Abstract

Previous studies of animal models of chronic mechanical compression of the spinal cord have mainly focused on cervical and thoracic lesions, but few studies have investigated thoracolumbar injury. The specific pathophysiological mechanism of chronic thoracolumbar cord injury has not yet been elucidated. The purpose of this study was to improve animal models of chronic thoracolumbar cord compression using the progressive screw. A custom-designed flat plastic screw was implanted in the spinal cord between thoracic vertebrae 12 and lumbar 1 of rats. The screw was tightened one complete turn (0.5 mm) every 7 days for 4 weeks to create different levels of chronic spinal cord compression. Following insertion of the screw, there was a significant decline in motor function of the hind limbs, and severe stenosis of micro-computed tomography parameters in the spinal cord. Cortical somatosensory evoked potential amplitudes were reduced remarkably, and latencies were prolonged at 30 minutes after surgery. The loss of motor neurons in the gray matter was marked. Demyelination and cavitation were observed in the white matter. An appropriate rat model of chronic thoracolumbar cord compression was successfully created using the progressive screw compression method, which simulated spinal cord compression injury.

Key Words: nerve regeneration; spinal cord compression; chronic spinal cord injury; cortical somatosensory evoked potential; electrophysiology; micro-computed tomography; animal model; behavioral evaluation; Basso, Beattie and Bresnahan score; histopathology; neural regeneration

Introduction

Chronic mechanical compression of the spinal cord is a common cause of neurological disability among the elderly. It is commonly caused by disc herniation, calcification of the posterior longitudinal ligaments, ossification of the yellow ligaments, tumors, and spinal deformities, all of which result in myelopathy and the insidious and progressive impairment of motor and sensory functions (Chagas et al., 2005).

The specific pathophysiological mechanisms of chron- ic spinal cord compression remain to be elucidated, but circulatory insufficiency leading to ischemia has been suggested as a possible contributor to neural degeneration (Karadimas et al., 2010; Kalsi-Ryan et al., 2012). Histo- logical examination of spinal cord of cervical spondylotic myelopathy patients showed a loss of motor neurons and vascular degeneration in the gray matter, as well as de- myelination and cavitation of axons in the white matter (Barnes and Saunders, 1984).

To better understand the pathophysiology of myelopathy, attempts have been made to reproduce these mechanisms in animal models using transection, contusion or compression methods (Rosenzweig and McDonald, 2004). These previous models used inflatable balloons (Lonjon et al., 2010), absorbent materials (Kim et al., 2004), and spinal movement (Kubota et al., 2011). Hukuda and Wilson (1972) placed subdural screws through the anterior vertebral body, then tightened the screws by approximately 1 mm daily, until the appearance of signs of neurological dysfunction. The impairment achieved in this model was the result of a subacute phase of compression injury. Since then, many authors (Al-Mefty et al., 1993; Lee et al., 2012) have suggested ways to improve the model. To precisely measure the depth of the screw insertion, Lee et al. (2012) designed a titanium-screw-based chronic compression internal fixation device that was fixed between the spinous processes of C_2 and T_2 *via* the posterior approach; the screws were fixed on the rod between the spinous processes, which increased the stability and accuracy of screw insertion. However, metal artifacts from the titanium screws affected postoperative imaging.

Surgical procedures of progressive screw implantation to obtain animal models of chronic spinal compression injury are simple and have good reproducibility (Kanchiku et al., 2001; Lee et al., 2012). Previous studies of chronic spinal cord compression mainly focused on cervical and thoracic spinal injury (Kim et al., 2004; Rosenzweig and McDonald, 2004; Lonjon et al., 2010; Lee et al., 2012); however, few studies have examined thoracolumbar spinal cord compression.

Therefore, the purpose of this study was to develop a novel rat model of chronic progressive thoracolumbar spinal cord compression. A custom-designed flat plastic screw was implanted in the spinal cord between T_{12} and L_1. The screw was tightened one complete turn to create different levels of chronic spinal cord compression. This novel rat model was evaluated using motor function assessment, micro-computed tomography (micro-CT), electrophysiological examination, and histopathological evaluation.

Materials and Methods

Animals

Forty-five mature and healthy Sprague-Dawley rats weighing 295 ± 25 g and aged 2 months old were provided by the Experimental Animal Center of the Chinese PLA General Hospital (SCXK2012-0001). The rats were kept in a controlled environment with free access to food and water. The 45 rats were randomized into a compression group ($n = 40$) and a control group ($n = 5$). The compression group was subdivided into 1-, 2-, 3-, and 4-week injury groups ($n = 10$/subgroup) with respective advancement of the screws by 0.5 mm (one complete turn) weekly. The control group ($n = 5$) did not undergo screw compression. The 1- and 2-week injury groups were defined as mild compression and the 3- and 4-week injury groups as severe compression.

Chronic compression device

The compression device (Chinese PLA General Hospital, China) was a custom-designed flat plastic screw (pitch of 0.5 mm, diameter of 3 mm, and height of 9 mm). Based on previous measurements of the T_{12}–L_1 vertebrae of mature rats, the sagittal diameter of the thoracolumbar canal is 2.7–3.3 mm and the transverse diameter is 3.5–4.0 mm. The screw was then adjusted to be positioned in the spinal cord between T_{12} and L_1.

Surgical procedure

The animals underwent surgery for implantation of the plastic screw by a spinal surgeon (Xu et al., 2008). Rats were maintained in a quiet laboratory for 30 minutes. After intraperitoneal anesthetization with 10% chloral hydrate at 3.0 mL/kg, the rats were intramuscularly injected with penicillin (4×10^5 U/kg). After sterilization with 0.5% iodophor, the rat was fixed on an operation table in a prone position, skin preparation was performed at the surgical area, and a sterile dressing was placed in the thoracolumbar area. An incision was made in the middle of the thoracolumbar segment. The skin and subcutaneous tissues were sequentially incised. The muscles around the spinous process-vertebral plate were bluntly dissected and the spinous process of T_{13} was removed. The vertebral laminae were drilled with 2-mm Kirschner wire. The tunnel was expanded using 3-mm plat K-wire. The screw was tapped by a quadrangular screwdriver (**Figure 1A–D**). During advancement of the screw (polyethylene, high-strength and no-distortion; Sheng Huang Technology Co., Ltd., Beijing, China), cortical somatosensory evoked potential (CSEP) was monitored. Establishment of the model was considered successful when the amplitude was decreased to 20–30% of the normal value, and the latency was prolonged < 10%. In the control group, the tunnel was expanded only, without insertion of the plastic screw. The peripheral muscles were sutured layer by layer. One week after surgery, a second compression was made. The screw cap was located in subcutaneous tissues, and the screw was turned a complete turn (0.5 mm). The same procedures were used for the third and fourth compressions.

Exclusion criteria for animals with acute spinal cord injury intraoperation and post-operation included: (1) the laminae cortex was obviously pushed forwards when the K-wire was drilled intraoperatively; (2) amplitude of CSEP was decreased by more than 50% during operation; and (3) when motor dysfunction of hind limbs assessed by Basso, Beattie and Bresnahan (BBB) score (Basso et al., 1995) indicated acute injury.

Electrophysiological evaluations

Rats were fixed on an operating table and connected to a Cascade Elite sensory evoked potential instrument (Cadwell Laboratories Inc., Kennewick, WA, USA). The stimulating electrodes (needle-like platinum electrodes) were placed on the fibular head, with a reference electrode located 1 cm subcutaneously. A constant current square pulse wave with a frequency of 2.7 Hz and pulse width of 0.2 ms was used to stimulate the tibial nerve. The stimulating current had appropriate strength (2.4–4.0 mA) to induce a contraction

of the gastrocnemius. The recording electrode was placed on rat skull at Cz-Fz, which is located 3 mm posterior to the intersection of the coronal and sagittal sutures, and a reference electrode was placed 1 cm below the recording electrode subcutaneously . Signals were amplified 100,000 times by two amplifiers (National Instruments Inc., Austin, TX, USA) and the frequency of signal filtering was 2–2,000 Hz. The resolution of data collection was 12 bit. Original signals were superimposed 200 times to obtain correct CSEP data (Hu et al., 2011).

CSEP was continuously monitored in each rat when the screw was inserted. The insertion was stopped when the amplitude was decreased to 20–30% of the normal value, the latency was prolonged < 10%, the observation lasted for 30 minutes, and there was no obvious sign of amplitude restoration. Compression injury was successful in rats without paralysis after they were awakened.

Behavioral evaluations
BBB Locomotor Rating Scale (Basso et al., 1995) was used to assess the recovery of motor function every week postoperatively. All rats were sacrificed 8 weeks after surgery. BBB scores were evaluated using the double-blind method, *i.e.*, the two hind limbs were observed by different staff members. BBB scores were ranked based on the sequence of locomotor patterns. A score of 0 indicated no spontaneous movement and a score of 21 indicated normal locomotion.

Micro-CT
All animals were anesthetized with 10% chloral hydrate at 3.0 mL/kg and sacrificed after 8 weeks. The rats were heparinized at 1:500,000, then the chest was opened, and the pericardium was incised longitudinally. An infusion catheter was immediately inserted and fixed in the aortic arch. Normal saline was perfused. An incision in the right atrium was made with an ophthalmic scissor for bloodletting until the effluent liquid became colorless and transparent. Afterwards, 4% paraformaldehyde was perfused to fix the samples. The whole sampling process took approximately 25 minutes. Centering on the screws, spinal cords from T_{10} to L_2 were harvested and fixed in 10% paraformaldehyde for 48 hours.

Micro-CT examination was performed as described previously (Hu et al., 2011). Samples were soaked in iodine reagent (iohexol, 15 g/50 mL) diluted with phosphate buffer (1:1) for 1 hour. The samples were fixed with a plastic tube and placed in the micro-CT scanner (GE Healthcare Inc., Ontario, Canada), with the longitudinal axis of the spinal cord parallel to the sliding track. Two samples were scanned simultaneously. Resolution was 47 μm. A single scanning took 14 minutes. X-ray tube voltage was 80 kV, filterability index was 1, and effective body element was 0.046 mm. Continuous scanning was conducted to reconstruct the three-dimensional images of rat spinal cord.

One hundred micro-CT scan layers, with the epicenter of cord compression, were selected from one vertebral body after the micro-CT was calibrated with a standard phantom.

The gray-scale value of each pixel in specimen images was calculated. Coloration was enhanced in the spinal cord within the region of interest to reconstruct the spinal cord with a screw (**Figure 2A**). According to the micro-CT observation, three parameters were calculated (Fehlings et al., 1999; Lee et al., 2012): (1) changes in CT height defined as the distance between the posterior margin of the vertebral body and the bottom of the plastic plate on the axial CT image (**Figure 2B**); (2) CT compression ratio (**Figure 2C**) determined on midsagittal images and calculated as CT compression ratio (%) = $1 - (c/(a+b)/2) \times 100\%$, where c is the anteroposterior canal diameter under maximum compression, and a and b are the anteroposterior canal diameters above and below and closest to the site of compression; and (3) the total canal cross-sectional area measured on the axial images, and containing areas from the posterior vertebra, bilateral vertebral plate, and bases of the spinous processes (Vaccaro et al., 2001; Keynan et al., 2006). The total vertebral canal cross-sectional area was calculated as $0.8 \times [\varpi (0.5 \text{ MSD} \times 0.5 \text{ TD})] + 0.1$, where MSD is the midsagittal diameter and TD is the maximal cross-sectional diameter. Data were analyzed with Micro-view software (version 2.2; GE Healthcare Inc.), and an average of three measurements was used for statistical analysis.

Histological examinations
After micro-CT scanning, the plastic screws and the tissues surrounding the screws were carefully removed, and the integrity of the spine was maintained. All the spinal cord from T_{10} to L_2 was removed. The samples were dehydrated through a series of graded alcohols and embedded in paraffin. Paraffin sections (7 μm) were cut. Transverse sections were used for hematoxylin-eosin staining, and longitudinal sections for Luxol fast blue staining.

Statistical analysis
Data are presented as the mean ± SD, and analyzed with SPSS 17.0 software (SPSS, Chicago, IL, USA). One-way analysis of variance was performed to analyze the BBB score and micro-CT measurement parameters. Least significant difference of *post hoc* multiple comparisons was used for data analysis among multiple groups. Paired *t*-tests were conducted for CSEP amplitudes and latencies between operation and post-operation. The α level was set at 0.05.

Results
Chronic spinal cord compression affected the cortical somatosensory evoked potentials
Typical changes of CSEP latencies and amplitudes were shown during operation (**Figure 3A–D**). No significant differences in latencies and amplitudes were observed in the control group. Amplitudes were significantly decreased 30 minutes post-operation in the 1- and 2-week injury groups, compared with the intraoperative period ($P < 0.05$). Latencies were significantly prolonged in the 3- and 4-week injury groups 30 minutes post-operation compared with the intraoperative period (**Figure 4A, B**).
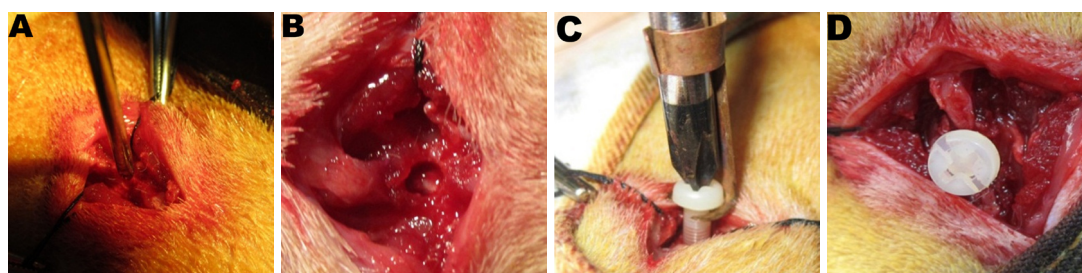
Figure 1 Experimental procedure of a rat model of spinal cord compression.
(A) The vertebral laminae were drilled through with Kirschner wire at T_{13}. (B) The 3-mm tunnel was the same as the screw diameter. (C) A plastic screw was tapped by a quadrangular screwdriver. (D) The position of the screw was on the T_{13} vertebral laminae.
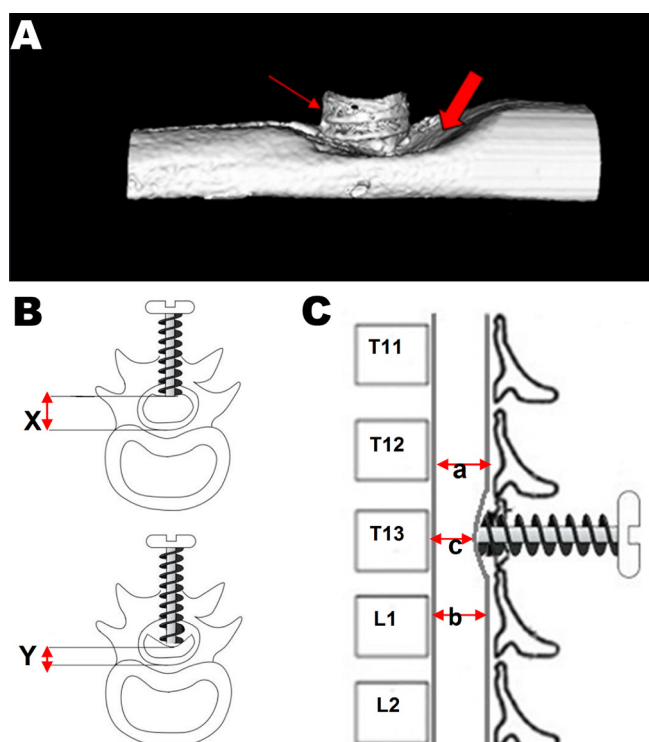
Figure 2 Three-dimensional reconstruction and parameter measurements on micro-CT images.
(A) Micro-CT three-dimensional reconstruction of the region of interest including rat spinal cord and screw. Red thick arrow indicates distortion of spinal cord compression, and red thin arrow indicates screw thread. (B) CT height was the distance between the posterior margin of the vertebral body and the bottom of the plastic plate on the axial CT image. CT height change = X−Y. (C) CT compression ratio was calculated in the median sagittal position, where c is the maximum compression level of the spinal canal sagittal diameter, and a and b are the distances of the upper and lower levels of the upper and lower vertebral canal sagittal diameter, respectively.

Figure 3 Typical latency and amplitude changes of cortical somatosensory evoked potentials during surgery.
(A) Normal changes of electromyogram in rats. (B) The latencies were significantly prolonged and the amplitudes were normal. (C) The latencies were normal, but the amplitudes were markedly decreased. (D) The latencies were significantly prolonged and the amplitudes were markedly decreased.

Micro-CT images in a rat model of chronic spinal cord compression

CT height and cross-sectional areas on axial views indicated compression of the vertebral canal. CT height and cross-sectional area in the control group were 2.99 ± 0.15 mm^2 and 7.46 ± 0.45 mm^2, respectively. In the compression group, CT height and cross-sectional area were gradually decreased. There were significant differences in these parameters among the different groups (**Figure 5A, B**; $P < 0.05$).

The compression ratio reflected changes of the spinal cord in response to screw compression based on the normal vertebral bodies above and below the site of compression. The compression ratios in the sagittal views of different groups were significantly increased ($P < 0.01$). Following insertion of the screws, the CT compression ratio was significantly more severe in weeks 3 and 4 after injury compared with weeks 1 and 2 (**Figure 5C, D**).

Recovery of neurological function in rats with chronic progressive spinal cord compression

Movements of the hind limbs of the 40 rats in the compression group were decreased with increasing screw compression. Rats with spinal cord injury manifested slow and uncoordinated movements. The five rats in the control group did not show obvious dysfunctions. BBB scores were significantly lower in the 3- and 4-week injury groups compared with the 1- and 2-week injury groups from weeks 5 to 8 ($P < 0.05$; **Figure 6**).
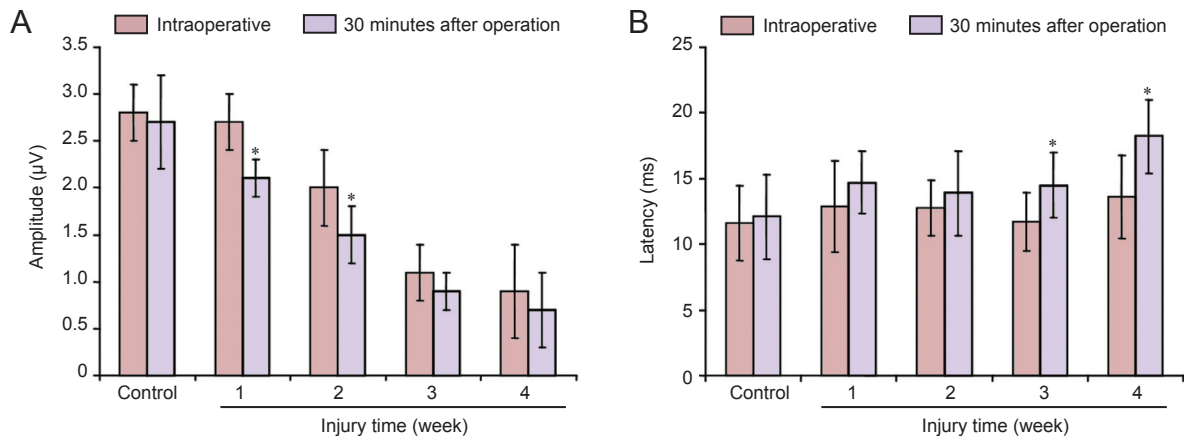
Figure 4 Changes in cortical somatosensory evoked potentials 30 minutes after operation in the 1-, 2-, 3-, and 4-week injury groups.
Changes of amplitudes (A) and latencies (B) in the intraoperative period and 30 minutes after operation in the 1-, 2-, 3-, and 4-week injury groups.
*$P < 0.05$, *vs.* intraoperative period. Data are presented as the mean ± SD (1-, 2-, 3-, and 4-week injury groups: $n = 10$/subgroup; control group: $n = 5$). Intergroup comparison was conducted with paired *t*-test between intraoperative period and 30 minutes post-operation.
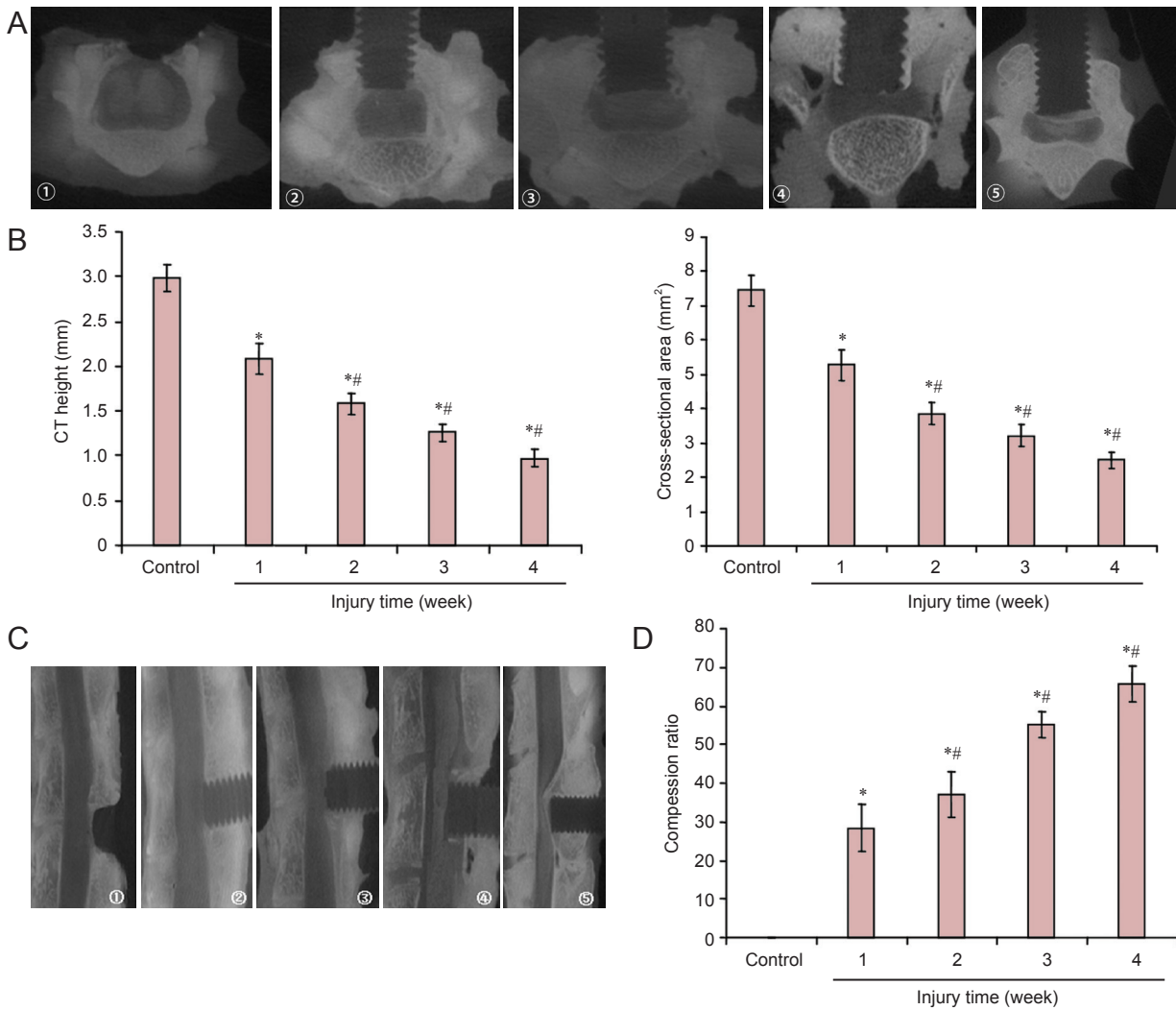
Figure 5 Measurement of micro-CT parameters on the axial and sagittal images of the model rats of spinal cord compression.
(A) Changes in the axial images among different groups. (B) CT height and total cross-sectional area of different groups. (C) Changes in the sagittal images among different groups. The compression of the spinal cord was evident with insertion of the screw. (D) CT compression ratio of different groups. Data are presented as the mean ± SD (1-, 2-, 3-, and 4-week injury groups: $n = 10$/subgroup; control group: $n = 5$). Measurement data were compared between different groups using one-way analysis of variance and least significant difference of *post hoc* multiple comparisons. *$P < 0.05$, *vs.* control group; #$P < 0.05$, *vs.* the prior time points. ① – ⑤ : Control group, 1-, 2-, 3-, 4-week injury groups, respectively.

Histopathological outcomes in rats with chronic progressive spinal cord compression

Increasing compression time led to progressive damage to the spine in the model rats. In the control group, the morphology of the spinal cord was intact and its surface was smooth, without adhesion. There was no damage to the epidural fat or the posterior middle artery. Bleeding and edema were absent. Ependymal cells were well organized, the white matter was evenly distributed, and the morphology of the myelin was intact and well organized. At low-power magnification, a large amount of anterior horn neurons with multiple synapses surrounded by small glial cells was observed. At high-power magnification, small blue particles in the anterior spinal neurons indicated Nissl bodies (cellular rough endoplasmic reticulum) (**Figure 7A**, **B**).

Compared with the control group, slight damage to the spinal cord was seen in the 1- and 2-week injury groups. The spinal cord became compressed and flat, the transverse diameter was large, and there was a slight depression of the posterior spinal cord. Numbers of the anterior spinal cells in the gray matter were decreased, while some cells bodies shrunk and/or were distorted and the number of synapses was reduced. There were also clefts around the nerve cells. Posterolateral fibers were disorganized, with a small amount of patch-like demyelination changes and a few vacuoles (**Figure 7C**, **D**).

Compared with the control group, obvious damage to the spinal cord was observed in the 1-, 2-, 3- and 4-week injury groups. In the 3- and 4-week injury groups, compression at the dorsal spinal cord was evident and the spinal cord was markedly depressed. Local epidural fat disappeared. The nerve tissue at the posterior spinal cord was missing. The number of nerve cells in the gray matter was reduced, and some neurons were lost and formed vacuoles. Glial cells within the gray matter became reactively proliferating. Ependymal cells protruded into the central canal, partially resulting in canal blockage. There was marked demyelination in the white matter, and nerve fibers were disarranged. Axons were broken and there was slight blood congestion (**Figure 7E**, **F**).

Discussion

There are many approaches for the establishment of animal models of cervical and thoracic spinal injuries (Kim et al., 2004; Rosenzweig and McDonald, 2004; Lonjon et al., 2010; Lee et al., 2012; Bonay and Vinit, 2014; Martínez-Pérez et al,. 2015; Yoshizumi et al., 2016), but little research has been performed for thoracolumbar spinal injury. A previous model developed in the 1970s (Hukuda et al., 1972) involved the insertion of screws into the vertebral body *via* an anterior approach. After the initial insertion, the screw was advanced 1 mm each day until the animals showed signs of neurological dysfunctions. Because of the rapid advance of the screw, the spinal cord injury was more of a subacute compression injury model than a chronic model. Nevertheless, this approach has been widely used in the establishment of chronic spinal cord compression models. Therefore, the aim of this study was to improve the existing animal model of chronic spinal cord compression using the progressive screw method. Our results revealed that the spinal cord function was associated with the severity of spinal stenosis, changes of CSEP, behavioral evaluations and histopathological outcomes.

Somatosensory evoked potential reflects the status of the posterior column of the spinal cord. If the corticospinal tract is damaged (located at the lateral cord) and the posterior funiculus of the spinal cord remains intact, somatosensory evoked potentials are not affected. Somatosensory evoked potential is a comprehensive action-potential activity induced by continuous stimulation of sensory nerve fibers at any region of the central nervous system, including CSEP and spinal somatosensory evoked potential. It is generally thought that CSEP depends on the integrity of the posterior funiculus and dorsolateral fasciculus, and reflects sensory functions of the spinal cord. Clinically, CSEP was first introduced for surgical monitoring and possesses advantages over the use of conventional intraoperative wake-up tests (Epstein et al., 1993). Change of amplitude is a sensitive and reliable index of acute spinal cord injury at the early stage of damage (Cheung et al., 2008; Hu et al., 2008). Moreover, CSEP has a low sensitivity for spinal cord compression, but prolonged latency indicates irreversible ultrastructural changes of the spinal cord (Hu et al., 2011). In this study, changes in latency and amplitude were concordant with chronic spinal cord injury, and these parameters worsened over time with advanced screw compression. A plastic screw was used, which did not affect postoperative imaging, compared with models using metal screws (Lee et al., 2012). CT height of axial images, transverse area of the vertebral canal, and CT compression rate in midsagittal views are three reliable parameters to evaluate canal compression (Kim et al., 2004; Plotino et al., 2006; Hu et al., 2011). In this study, the severity of stenosis by micro-CT parameters was consistent with the amount of compression applied by the screws.

Behavioral changes, canal compression (micro-CT measurement parameters), and changes of intraoperative CSEP are associated with histopathological changes. The histological findings in our study, including the loss of motor neurons of gray matter, demyelination and cavitation of white matter, were consistent with a previous study on chronic compression of spinal cord (Kraus, 1996). There was similar functional and histological change in the rat model with the chronic compression of clinical patients. Our data indicate that this model results in chronic and precise thoracolumbar cord compression. The measurable deficits seen in neurological measurements will be useful for evaluating the therapeutic efficacy of decompressive surgery and other treatment approaches. A novel animal model of chronic thoracolumbar spinal cord compression was created by progressive screw compression with a CT-compatible plastic screw. Changes in the dysfunction of the spinal cord, degree of canal compression, CSEP, neurobehavioral assessment, and histopathology were significant and progressive over time. This model is a clinically relevant useful animal model for investigating thoracolumbar spinal cord compression, which may provide
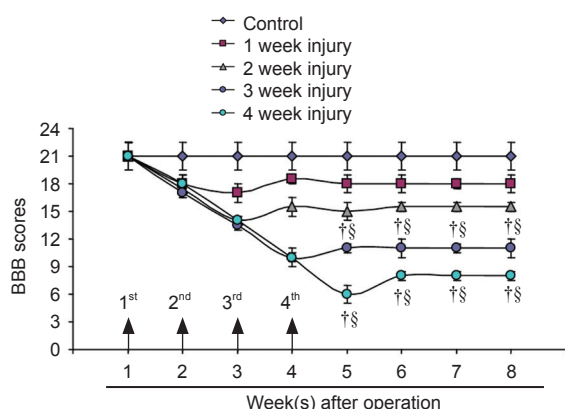
Figure 6 Changes of neurological function in rats with chronic progressive spinal cord compression.
BBB score was used to assess the recovery of motor function every week postoperatively (0 indicated no spontaneous movement, 21 indicated normal locomotion). Data are presented as the mean ± SD (1-, 2-, 3-, and 4-week injury groups: $n = 10$/subgroup; control group: $n = 5$). Measurement data were compared between different groups using one-way analysis of variance and the least significant difference of *post hoc* multiple comparisons. †$P < 0.05$, *vs.* 1-week injury group, §$P < 0.05$, *vs.* 2-week injury group. BBB: Basso, Beattie and Bresnahan locomotor rating scale.
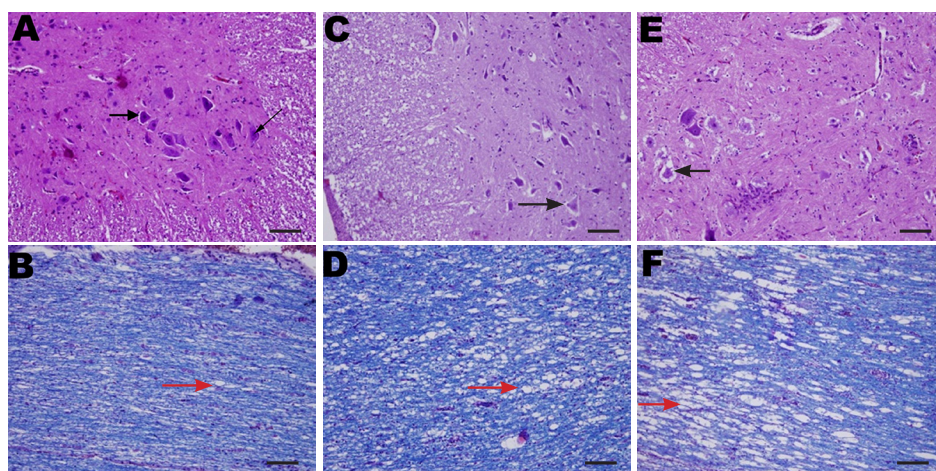
Figure 7 Spinal cord histopathology in different groups with hematoxylin-eosin staining and Luxol blue staining.
(A–B) Control group. (A) Hematoxylin-eosin staining: Polysynaptic neurons (black arrows) are present in the anterior horn of the spinal cord. (B) Blue-stained particles (Nissl bodies, red arrow) are distributed in the nuclei. Luxol fast blue staining indicates that the morphology of peripheral myelin is intact with regular arrangement and no evident vacuoles. (C–D) 1- and 2-week injury groups. (C) Hematoxylin-eosin staining: the number of spinal anterior horn cells (black arrow) and synapses is decreased; some cells have shrunk and are deformed. (D) Luxol blue staining: disordered structure of posterolateral fibers and small cavitation (red arrow). (E–F) 3- and 4-week injury groups. (E) Hematoxylin-eosin staining: the volume of the spinal anterior horn cells (black arrow) is reduced, and large vacuoles are present between the anterior horn cells and the surrounding tissues. (F) Luxol blue staining: disordered structure of posterolateral fibers of the white matter and large cavitation (red arrow). Scale bars: 100 μm.

experimental data for determining the time of surgical decompression.

This study had some limitations. Only four levels of compression were observed. Histopathological analysis was not used to quantify the cells, but crude outcomes were obtained by morphology and microscope scans. In addition, long-term follow-up of animals was not performed. Further studies are necessary to improve this model.

Author contributions: *YS contributed to study design, paper preparation and drafting the paper. LHZ, YMF, ZRL, JHL, JP and BL performed experiments, participated in data collection and data analysis. PFT revised the paper for important contents. All authors approved the final version of the paper.*
Conflicts of interest: *None declared.*
Plagiarism check: *This paper was screened twice using Cross-Check to verify originality before publication.*

Peer review: *This paper was double-blinded and stringently reviewed by international expert reviewers.*

References

Al-Mefty O, Harkey HL, Marawi I, Haines DE, Peeler DF, Wilner HI, Smith RR, Holaday HR, Haining JL, Russell WF (1993) Experimental chronic compressive cervical myelopathy. J Neurosurg 79:550-561.

Barnes M, Saunders M (1984) The effect of cervical mobility on the natural history of cervical spondylotic myelopathy. J Neurol Neurosurg Psychiatry 47:17-20.

Basso DM, Beattie MS, Bresnahan JC (1995) A sensitive and reliable locomotor rating scale for open field testing in rats. J Neurotrauma 12:1-21.

Bonay M, Vinit S (2014) New perspectives for investigating respiratory failure induced by cervical spinal cord injury. Neural Regen Res 9:1949-1951.

Chagas H, Domingues F, Aversa A, Fonseca ALV, de Souza JM (2005) Cervical spondylotic myelopathy: 10 years of prospective outcome analysis of anterior decompression and fusion. Surg Neurol 64:S30-35.

Cheung W, Arvinte D, Wong Y, Luk K, Cheung K (2008) Neurological recovery after surgical decompression in patients with cervical spondylotic myelopathy-a prospective study. Int Orthop 32:273-278.

Epstein NE, Danto J, Nardi D (1993) Evaluation of intraoperative somatosensory-evoked potential monitoring during 100 cervical operations. Spine 18:737-747.

Fehlings MG, Rao SC, Tator CH, Skaf G, Arnold P, Benzel E, Dickman C, Cuddy B, Green B, Hitchon P (1999) The optimal radiologic method for assessing spinal canal compromise and cord compression in patients with cervical spinal cord injury: Part II: results of a multicenter study. Spine 24:605-613.

Hu Y, Ding Y, Ruan D, Wong YW, Cheung KM, Luk KD (2008) Prognostic value of somatosensory-evoked potentials in the surgical management of cervical spondylotic myelopathy. Spine 33:E305-310.

Hu Y, Wen CY, Li T, Cheung MM, Wu EX, Luk KD (2011) Somatosensory-evoked potentials as an indicator for the extent of ultrastructural damage of the spinal cord after chronic compressive injuries in a rat model. Clin Neurophysiol 122:1440-1447.

Hukuda S, Wilson CB (1972) Experimental cervical myelopathy: effects of compression and ischemia on the canine cervical cord. J Neurosurg 37:631-652.

Kalsi-Ryan S, Karadimas SK, Fehlings MG (2012) Cervical spondylotic myelopathy the clinical phenomenon and the current pathobiology of an increasingly prevalent and devastating disorder. Neuroscientist 19:409-421

Kanchiku T, Taguchi T, Kaneko K, Yonemura H, Kawai S, Gondo T (2001) A new rabbit model for the study on cervical compressive myelopathy. J Orthop Res 19:605-613.

Karadimas S, Gialeli C, Klironomos G. Tzanakakis G, Panagiotopoulos E, Karamanos N, Gatzounis G (2010) The role of oligodendrocytes in the molecular pathobiology and potential molecular treatment of cervical spondylotic myelopathy. Curr Med Chem 17:1048-1058.

Keynan O, Fisher CG, Vaccaro A, Fehlings MG, Oner FC, Dietz J, Kwon B, Rampersaud R, Bono C, France J (2006) Radiographic measurement parameters in thoracolumbar fractures: a systematic review and consensus statement of the spine trauma study group. Spine 31: E156-165.

Kim P, Haisa T, Kawamoto T, Kirino T, Wakai S (2004) Delayed myelopathy induced by chronic compression in the rat spinal cord. Ann Neurol 55:503-511.

Kraus KH (1996) The pathophysiology of spinal cord injury and its clinical implications. Semin Vet Med Surg (Small Anim) 11:201-207.

Kubota M, Kobayashi S, Nonoyama T, Shimada S, Takeno K, Miyazaki T, Guerrero AR, Iwamoto H, Baba H (2011) Development of a chronic cervical cord compression model in rats: changes in the neurological behaviors and radiological and pathological findings. J Neurotrauma 28:459-467.

Lee J, Satkunendrarajah K, Fehlings MG (2012) Development and characterization of a novel rat model of cervical spondylotic myelopathy: the impact of chronic cord compression on clinical, neuroanatomical, and neurophysiological outcomes. J Neurotrauma 29:1012-1027.

Lonjon N, Kouyoumdjian P, Prieto M, Bauchet L, Haton H, Gaviria M, Privat A, Perrin FE (2010) Early functional outcomes and histological analysis after spinal cord compression injury in rats: Laboratory investigation. J Neurosurg Spine 12:106-113.

Martínez-Pérez R, Fuentes F, Alemany VS (2015) Subaxial cervical spine injury classification system: is it most appropriate for classifying cervical injury? Neural Regen Res 10:1416-1417.

Plotino G, Grande NM, Pecci R, Bedini R, Pameijer CH, Somma F (2006) Three-dimensional imaging using microcomputed tomography for studying tooth macromorphology. J Am Dent Assoc 37:1555-1561.

Rosenzweig ES, McDonald JW (2004) Rodent models for treatment of spinal cord injury: research trends and progress toward useful repair. Curr Opin Neurol 17:121-131.

Vaccaro AR, Nachwalter RS, Klein GR, Sewards JM, Albert TJ, Garfin SR (2001). The significance of thoracolumbar spinal canal size in spinal cord injury patients. Spine 26:371-376.

Xu P, Gong WM, Li Y, Zhang T, Zhang K, Yin DZ, Jia TH (2008) Destructive pathological changes in the rat spinal cord due to chronic mechanical compression. J Neurosurg Spine 8:279-285.

Yoshizumi T, Murata H, Yamamoto S, Kurokawa R, Kim P, Kawahara N (2016) Granulocyte colony-stimulating factor improves motor function in rats developing compression myelopathy. Spine (Phila Pa 1976).